PMSM Rotor Speed and Position Estimator

Mohamed Azmi Said, W.P. Hew, N.A. Rahim
UM Power Energy Dedicated Advanced Centre (UMPEDAC)
Level 4, Engineering Tower, University of Malaya
50603 Kuala Lumpur
azmisaid@siswa.um.edu.my

Abstract — **Estimation techniques have been developed for flux observer, rotor position, and speed. The techniques have a common problem of the offset in voltage-sensor and current-sensor outputs increasing during integration, causing instability. This paper describes an attempt to overcome the problem through estimations of rotor position and speed of a permanent magnet synchronous motor (PMSM) by three methods: with cascaded low pass filter (LPF), with adaptive sensorless rotor flux observer, and with sliding mode observer (SMO). Simulation on Matlab/Simulink validated the proposed method. The advantages and drawbacks of each implementation are discussed.**

Keywords - PMSM motor drives, sensorless, cascaded LPF, adaptive rotor flux observer, SMO.

I. Introduction

Permanent magnet synchronous motor (PMSM) is popular for its high efficiency, high power density, very low inertia, and high reliability. In field-oriented control (FOC) or vector control schemes, continuous rotor information is mandatory. To ensure a PMSM's high performance and precise speed control, a position encoder is required; it senses and continuously feeds back both position and speed. The position encoder, though, imposes drawbacks on a system: it is costly, it complicates circuit, is sensitive to noise, and, in a hostile environment, is fragile [1]. Its absence is thus desired. Figure 1 is a block diagram of a sensorless PMSM vector control drive.

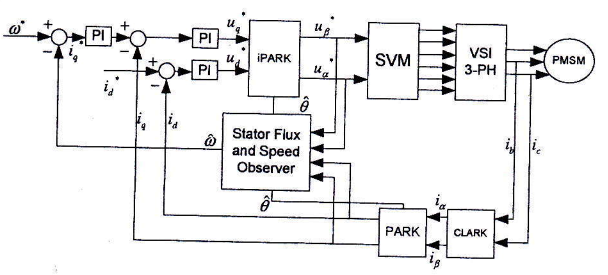

Figure 1: Sensorless vector control PMSM drive

Direct torque control (DTC) [2] is less parameter-dependent, has fast dynamic response, and does not need a mechanical rotor position sensor for its control loop. Problems exist, though, namely, drift in stator-flux-linkage estimation, owing to measurement offset error and varying stator resistance.

The stator flux linkage in DTC scheme is estimated by integrating the difference between input voltage and voltage drop across stator resistance:

$$\lambda_s = v_s t - R_s \int i_s dt + \lambda_{s|t=0} \tag{1}$$

Rotor flux linkage $\lambda_D(k)$ and $\lambda_Q(k)$ at the *k*th sampling are calculated from stator voltage and current:

$$\lambda_D(k) = \lambda_{D/k-1} + (V_{D/k-1} - R_s i_D)T_s \tag{2}$$

$$\lambda_Q(k) = \lambda_{Q/k-1} + (V_{Q/k-1} - R_s i_D)T_s \tag{3}$$

$$\lambda_s(k) = \sqrt{\lambda_D^2(k) + \lambda_Q^2(k)} \tag{4}$$

From (5), rotor position θ can be calculated as:

$$\theta = \tan^{-1}\left(\frac{\lambda_Q(k)}{\lambda_D(k)}\right) \tag{5}$$

Rotor position angle θ depends on estimated stator flux, which is determined by integrating the difference between input voltage and voltage drop across resistance, as Equation (1) shows. There is an offset error produced by current and voltage sensors. When stator flux is indirectly integrated, any dc offset error is also integrated. This eventually causes a large drift in stator flux estimation. The offset error is non-periodical and unidirectional. It can not be rectified by calculation alone. It must be overcome by some means of compensation (see Figure 7 for offset of flux locus).

A. *Flux estimator with a programmable cascaded low-pass filter*

Figure 2 is a block diagram of the three-stage programmable cascaded LPF [3]. The discrete transfer characteristic of an LPF is:

$$\frac{Y}{X} = \frac{1}{1 + \tau \frac{1 - z^{-1}}{T_s}} = \frac{T_s}{T_s + \tau(1 - z^{-1})} \tag{6}$$

where T_s is the sampling time and τ is the time constant. The corresponding difference equation is:

$$y(kT_s) = \frac{1}{T_s + \tau}[T_s x(kT_s) + \tau y(kT_s - T_s)] \tag{7}$$

τ and G are functions of frequency or the rotor speed, at steady state, and are calculated as follows:

$$\tau = \frac{\tan\left(\frac{90^0}{n}\right)}{\omega} \quad (8)$$

$$G = \frac{\left(\sqrt{[1+(\tau\omega)^2]}\right)^n}{\omega} \quad (9)$$

where n is the number of filters cascaded. When the signal is dc, τ and G become infinite, thus the filter cannot perform the integration. Implementation of the cascaded LPF allows the flux locus to remain centered on the origin.

The integration process however, requires knowledge of the initial stator flux position. If the initial-position information in the controller is inaccurate, the motor may initially rotate in the wrong direction. Cascaded LPF depends heavily too on motor frequency. At zero and very low speeds, its implementation draws a disadvantage.

B. *Adaptive sensorless rotor flux observer*

Adaptive sensorless rotor flux observer can be used to calculate rotor position and speed [4]. From Equation (1), the dynamics of a PMSM motor is given by the following stator voltage and flux linkage equation:

$$\frac{d\lambda_s}{dt} = v_s - R_s i_s \quad (10)$$

$$\lambda_s = L_s i_s + \lambda_r \quad (11)$$

$$\lambda_r = \lambda_M e^{j\theta} \quad (12)$$

where θ is the rotor angle. Electrical rotor speed is expressed from mechanical rotor speed:

$$\frac{d\theta}{dt} = \omega = p\,\omega_{mech} \quad (13)$$

Estimation of λ_r requires an open integration of the voltage equation. The offset contained in the inputs hence makes the output drift. The offset is modeled as $\hat{u}_{off}$. Estimator for the rotor flux is:

$$\frac{d\hat{\lambda}}{dt} = v_s - R_s i_s + \hat{u}_{off} \quad (14)$$

$$\lambda_r = \lambda_M e^{j\theta} \quad (15)$$

where $\hat{u}_{off}$ has to be designed in a way that leads to a flux estimate with constant amplitude $|\lambda_r|$.

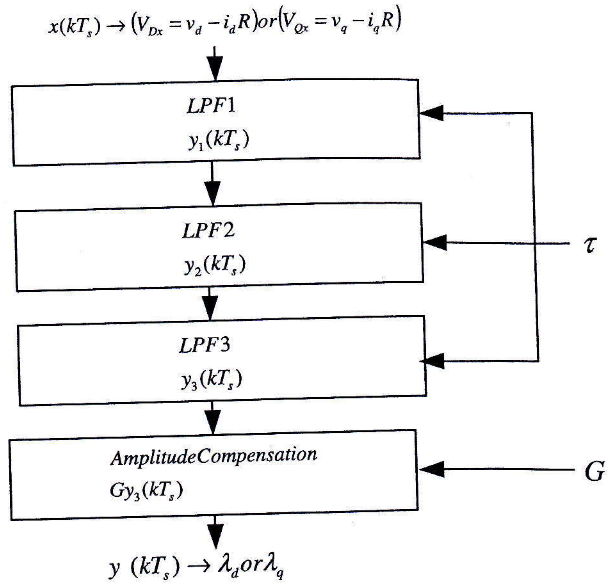

Figure 2: Block diagram of a three-stage programmable LPF

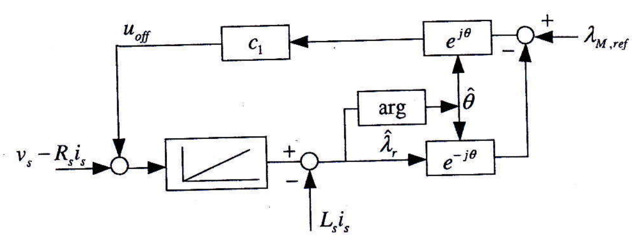

Figure 3: Signal flow graph of the rotor angle observer

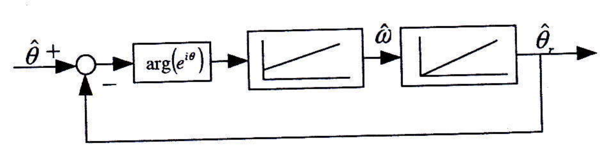

Figure 4: Speed estimator

Figure 3 shows how this is obtained by a feedback of the estimated error $\lambda_{M,ref} - \hat{\lambda}_M$. For a known magnitude of the permanent magnet, $\lambda_{M,ref} = \lambda_M$ is used. The observer may then be seen as a rotor field angle estimator. At zero and very low speeds, BEMF gives no information of the field angle. A new principle is introduced to the situation by impressing a current in the direction of the default estimated angle. The current then forces the permanent magnet to align to that angle; this way, the estimated angle becomes correct only with the error caused by friction and load.

Figure 4 shows the signal flow graph for the rotor speed estimator. The $\arg\left(e^{j\theta}\right)$ block solves the modulus problem. The algorithm for the estimator then becomes:

$$\frac{d\hat{\lambda}_s}{dt} = v_s - R_s i_s + c_1\left(\lambda_{M,ref} - \hat{\lambda}_M\right)e^{j\hat{\theta}} \quad (16)$$

$$\hat{\lambda}_r = \hat{\lambda}_s - L_s i_s \quad (17)$$

$$\hat{\theta} = \arg(\hat{\lambda}_r) \quad (18)$$

$$\hat{\omega} = K_p\left(1 - \frac{1}{T_i}\right)\arg e^{j(\hat{\theta}-\theta_f)} \quad (19)$$

$$\frac{d\hat{\theta}_f}{dt} = \hat{\omega} \quad (20)$$

C. *Sliding mode observer*

In sliding mode, the observers are insensitive to parameter variations and disturbance. Sliding mode observer has been presented for robust estimation of the state variable of controlled objects [5-7]. Compared with other methods, the observer is more robust to operating conditions and parameter uncertainties [8].

To estimate rotor position and angular speed of a PMSM, the motor is generally modeled in stationary reference frame. The angular speed and position information are ready to be extracted in this frame.

In stationary condition, $\alpha\beta$ reference frame can be written as:

$$\frac{di_\alpha}{dt} = -\frac{R}{L}i_\alpha - \frac{1}{L}e_\alpha + \frac{1}{L}v_\alpha \quad (21)$$

$$\frac{di_\beta}{dt} = -\frac{R}{L}i_\beta - \frac{1}{L}e_\beta + \frac{1}{L}v_\beta \quad (22)$$

$$e_\alpha = -\lambda_0\omega_e\sin(\theta_e) \quad (23)$$

$$e_\beta = \lambda_0\omega_e\cos(\theta_e) \quad (24)$$

The motor speed changes slowly, implying that $\dot{\omega} = 0$, the model for the induced back EMF is:

$$\dot{e}_\alpha = \omega_e e_\beta; \quad \dot{e}_\beta = \omega_e e_\alpha \quad (25)$$

The sliding mode observer uses only motor electrical equation. Its main equations are:

$$\frac{d\hat{i}_\alpha}{dt} = -\frac{R}{L}\hat{i}_\alpha - \frac{1}{L}v_\alpha + \frac{1}{L}sign\left(\bar{i}_\alpha\right) \quad (26)$$

$$\frac{d\hat{i}_\beta}{dt} = -\frac{R}{L}\hat{i}_\beta - \frac{1}{L}v_\beta + \frac{1}{L}sign\left(\bar{i}_\beta\right) \quad (27)$$

where l_1 is constant observer gain, and $\bar{i}_\alpha = \hat{i}_\alpha - i_\alpha$, $\bar{i}_\beta = \hat{i}_\beta - i_\beta$ are observer mismatches. Assuming that the motor parameters are identical with those in the model, the mismatch dynamics is:

$$\frac{d\bar{i}_\alpha}{dt} = -\frac{R}{L}\bar{i}_\alpha - \frac{1}{L}v_\alpha + \frac{1}{L}sign\left(\bar{i}_\alpha\right) \quad (28)$$

$$\frac{d\bar{i}_\beta}{dt} = -\frac{R}{L}\bar{i}_\beta - \frac{1}{L}v_\beta + \frac{1}{L}sign\left(\bar{i}_\beta\right) \quad (29)$$

The dynamics are distributed by the unknown induced EMF components. However, the back EMF components are bounded, so they may be suppressed by continuous input, with $l_1 > \max\left(|e_\alpha|,|e_\beta|\right)$. The sliding hyper plane on the stator current errors $S = x = \left[\bar{i}_\alpha \quad \bar{i}_\beta\right]^T$ is defined according to the sliding mode observer theory. The system behavior can be examined by applying equivalent control method, when the sliding mode occurs after a finite time interval $\bar{i}_\alpha = 0$ and $\bar{i}_\beta = 0$.

From Equations (21) and (22),

$$A = \begin{bmatrix} -\frac{R}{L} & 0 \\ 0 & -\frac{R}{L} \end{bmatrix}, \quad B = \begin{bmatrix} -1/L \\ -1/L \end{bmatrix} \quad (30)$$

Setting $\dot{\bar{i}}_\alpha = 0$, $\dot{\bar{i}}_\beta = 0$ gives:

$$u_{eq\alpha} = \left(l_1 sign\left(i_\alpha\right)\right)_{eq} = e_\alpha \quad (31)$$

$$u_{eq\alpha} = \left(l_1 sign\left(i_\alpha\right)\right)_{eq} = e_\alpha \quad (32)$$

To extract e_α and e_β from the corresponding equivalent control values, a low pass filter is used with z_α, z_β as filter outputs:

$$z_\alpha(t) = e_\alpha(t) + \Delta_u(t) \quad (33)$$

$$z_\beta(t) = e_\beta(t) + \Delta_u(t) \quad (34)$$

z_β can not be used directly. Equations (33) and (34) are used for better filtering and estimate the rotor angular speed and position. The observer undertaking the filtering task is:

$$\dot{\hat{e}}_\alpha = -\hat{\omega}_e e_\beta - l_2\left(\hat{e}_\alpha - z_\alpha\right) \quad (35)$$

$$\dot{\hat{e}}_\beta = \hat{\omega}_e e_\alpha - l_2\left(\hat{e}_\beta - z_\beta\right) \quad (36)$$

$$\dot{\hat{\omega}}_e = \left(\hat{e}_\alpha - z_\alpha\right)e_\beta - \left(\hat{e}_\beta - z_\beta\right)\hat{e}_\alpha \quad (37)$$

where l_2 is a constant observer gain. Mismatches in the back EMF equations are:

$$\dot{\bar{e}}_\alpha = -\hat{\omega}_e\hat{e}_\beta + \omega_e e_\beta - l_2\left(\hat{e}_\alpha - e_\alpha\right) \quad (38)$$

$$\dot{\bar{e}}_\beta = \hat{\omega}_e e_\alpha - \omega_e e_\alpha - l_2\left(\hat{e}_\beta - e_\beta\right) \quad (39)$$

$$\dot{\bar{\omega}}_e = \left(\hat{e}_\alpha - e_\alpha\right)\hat{e}_\beta - \left(\hat{e}_\beta - e_\beta\right)\hat{e}_\alpha \quad (40)$$

where $\bar{e}_\alpha = \hat{e}_\alpha - e_\alpha$, $\bar{e}_\beta = \hat{e}_\beta - e_\beta$, $\bar{\omega}_e = \hat{\omega}_e - \omega_e$ are observer errors. According to relations in (21) and (22),

$$\hat{e}_\alpha = -\lambda_0\omega_e\sin\left(\hat{\theta}_e\right) \quad (41)$$

$$\hat{e}_\alpha = -\lambda_0 \omega_e \sin\left(\hat{\theta}_e\right) \tag{42}$$

$\sin\left(\hat{\theta}_e\right)$ and $\cos\left(\hat{\theta}_e\right)$ can be obtained as:

$$\sin\left(\hat{\theta}_e\right) = -\frac{1}{\lambda_0}\frac{\hat{e}_\alpha}{\omega_e} \tag{43}$$

$$\cos\left(\hat{\theta}_e\right) = \frac{1}{\lambda_0}\frac{\hat{e}_\beta}{\omega_e} \tag{44}$$

The *signal flow* diagram for sliding mode observer can be implemented as shown in Figure 5.

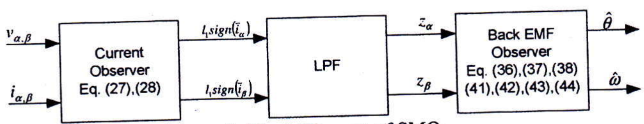

Figure 5: Block Diagram of SMO

II. RESULTS

The observer behaviors were tested in Matlab/Simulink software simulation tool. Parameters of the PMSM model are as tabulated in Table I.

TABLE IV. DATA OF PMSM

Number of pole pairs	p	8
Armature resistance	R	1.1 Ω
Magnet flux linkage	λ	0.28 Wb
d-axis inductance	L_d	8.65 mH
q-axis inductance	L_q	8.65 mH
Inertia	J	0.0051 kg.m^2
Friction factor	F	0.0050 N.m.s

In sensorless drive operation, the estimated stator flux is used to calculate torque, flux, and rotor position. DTC drive implementation requires all three observer outputs as feedbacks to closed-loop control. Meanwhile, FOC drive need position feedback to transform the stator current measured from stationary reference $\alpha\beta$ frame to rotating reference frame dq.

Figure 6 shows the flux locus calculated from an ideal input stator current without the presence of dc offset. In actual implementation, with an offset measurement present, there is a drift in stator flux locus, caused by the offset error in flux linkage estimation.

Cascaded LPF will compensate the offset error; see Figure 8. A filter resets the integrator used in estimating the stator flux linkage. The flux locus is seen to remain centered on the origin. It clearly starts from the origin, requiring an initial rotor position. The observer also depends on motor frequency ω, requiring the motor to run at some speed first before the cascaded LPF can be implemented.

As Figure 9 shows, adaptive sensorless rotor flux observer can be operated from zero speed. The switch from open-loop control for start up to closed loop can be full of noise and give extreme speed transients. Adaptive sensorless operates from zero speed without changing the control structure.

SMO simulation results show accurate speed and position estimation. Figures 10 and 11 show the actual and the estimated angles. The position angle error as shown in Figure 12 is under 0.015p.u, below 5 degrees of electrical angle.

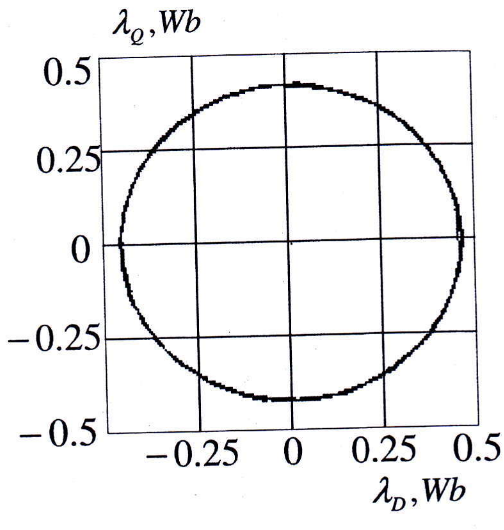

Figure 6: Flux locus for ideal measurement of current and voltage without dc offset.

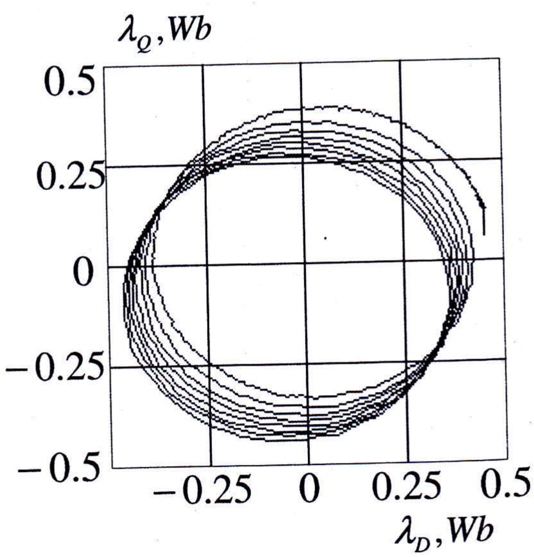

Figure 7: Flux locus with stator current measurement considering dc offset.

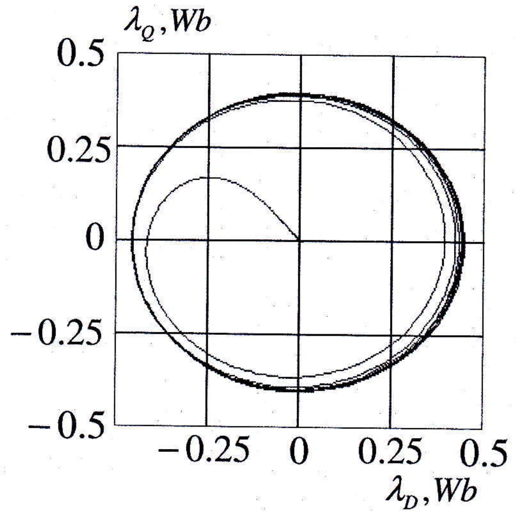

Figure 8: Flux locus calculated by using flux estimator with programmable cascaded low-pass filter

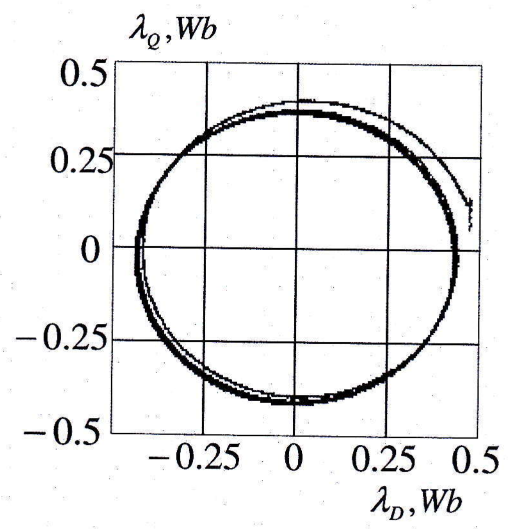

Figure 9: Flux locus calculated based on active rotor flux observer. However, at zero and low speeds, adaptive sensorless requires a non-zero i_{sd} reference value.

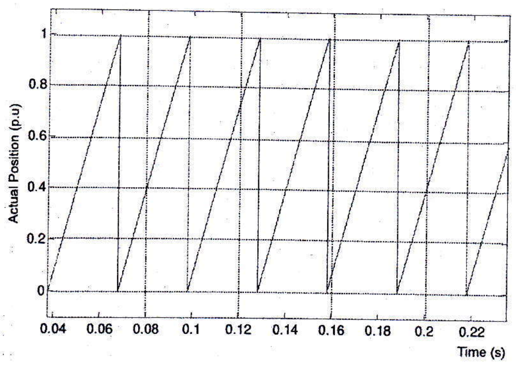

Figure 10: Actual rotor position angle

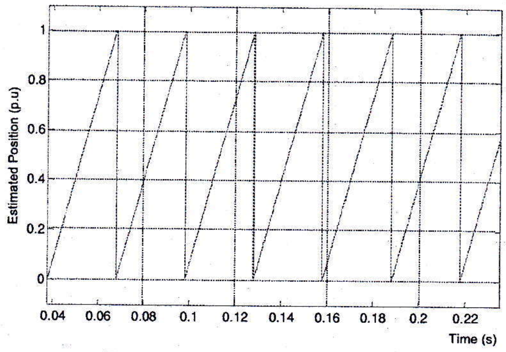

Figure 11: SMO estimated position

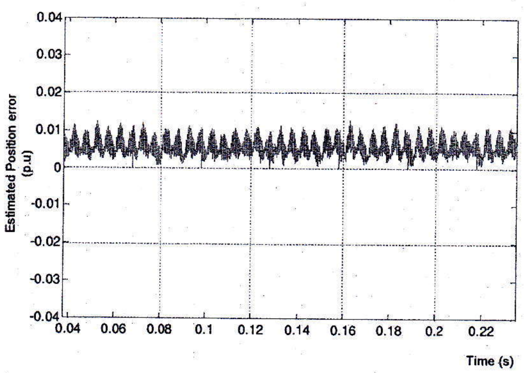

Figure 12: SMO position estimation error

III. Conclusions

Offset error due to the presence of dc in stator current and voltage measurement in PMSM motor drive causes drifts in stator-flux calculation, in turn causing inaccurate estimation of rotor angle position. Cascaded LPF is able to diminish the drift but the calculation is assumed running at steady state. Adaptive sensorless rotor flux observer may be used at zero or low speeds but the current reference must be set to a non-zero value initially. SMO can calculate rotor position angle accurately, with low position-error.

Acknowledgment

The support of UM Power Energy Dedicated Advanced Centre (UMPEDAC) is gratefully acknowledged. M.A. Said's research study is funded by Universiti Teknikal Malaysia Melaka.

(Text edited by wirani_umpedac@yahoo.com)

References

[1] T. Lixin, Z. Limin, M.F. Rahman, and Y. Hu, "A novel direct torque controlled interior permanent magnet synchronous machine drive with low ripple in flux and torque and fixed switching frequency," *Power Electronics, IEEE Transactions on,* vol. 19, pp. 346-354, 2004.

[2] I. Takahashi and T. Noguchi, "A New Quick-Response and High-Efficiency Control Strategy of an Induction Motor," *Industry Applications, IEEE Transactions on,* vol. IA-22, pp. 820-827, 1986.

[3] M.F. Rahman, M.E. Haque, T. Lixin, and Z. Limin, "Problems associated with the direct torque control of

an interior permanent-magnet synchronous motor drive and their remedies," *Industrial Electronics, IEEE Transactions on,* vol. 51, pp. 799-809, 2004.

[4] H. Rasmussen, P. Vadstrup, and H. Borsting, "Adaptive sensorless field oriented control of PM motors including zero speed," in *Industrial Electronics, 2004 IEEE International Symposium on*, 2004, pp. 1191-1196 vol. 2.

[5] L. Changsheng and M. Elbuluk, "A sliding mode observer for sensorless control of permanent magnet synchronous motors," in *Industry Applications Conference, 2001. Thirty-Sixth IAS Annual Meeting. Conference Record of the 2001 IEEE*, 2001, pp. 1273-1278 vol.2.

[6] J. Lee, J. Son, and H. Kim, "A High Speed Sliding Mode Observer for the Sensorless Speed Control of a PMSM," *Industrial Electronics, IEEE Transactions on,* vol. PP, pp. 1-1.

[7] G. Foo and M.F. Rahman, "Direct torque and flux controlled IPM synchronous motor drive using a hybrid signal injection and adaptive sliding mode observer," in *TENCON 2009 - 2009 IEEE Region 10 Conference*, 2009, pp. 1-7.

[8] J. Dong, Z. Zhengming, and W. Fei, "A Sliding Mode Observer for PMSM speed and rotor position considering saliency," in *Power Electronics Specialists Conference, 2008. PESC 2008. IEEE*, 2008, pp. 809-814.